



GREEN SYNTHESIS OF ZINC OXIDE NANOPARTICLES USING *Swertia chirayita* FOR PHOTOCATALYTIC AND ANTIMICROBIAL ACTIVITY

Devendra Khadka^{1,2}, Praveen Bista³, Janaki Bara³, Surendra Kumar Gautam³, Bishnu Prasad Bastakoti⁴, Bhoj Raj Poudel^{3*}, Megh Raj Pokhrel¹

¹Central Department of Chemistry, Institute of Science and Technology, Tribhuvan University, Kirtipur, Kathmandu, Nepal

²Department of Chemistry, Tribhuvan Multiple Campus, Tribhuvan University, Tansen, Palpa, Nepal

³Department of Chemistry, Tri-Chandra Multiple Campus, Tribhuvan University, Ghantaghar, Kathmandu, Nepal

⁴Department of Chemistry, College of Science and Technology, North Carolina Agricultural and Technical State University, Greensboro USA

*Correspondence: bhoj.poudel@trv.tu.edu.np

(Received: December 05, 2024; Final Revision: February 25, 2025; Accepted: February 26, 2025)

ABSTRACT

This research work utilized an environmentally friendly and sustainable method to produce zinc oxide nanoparticles (ZnO NPs) using zinc nitrate as a precursor and the leaf extract of *Swertia chirayita*. The resulting nanoparticles were characterized using various analytical techniques, including UV-vis spectroscopy, X-ray diffraction (XRD), Fourier transform infrared (FTIR) spectroscopy, field emission scanning electron microscopy (FESEM), and energy-dispersive spectroscopy (EDS). The ZnO nanoparticles were found to have a well-defined crystalline structure, with their average crystallite size measured at around 10.88 nm. Agar well diffusion was used to study the antimicrobial activity, revealing notable antibacterial and antifungal properties, indicating broad-spectrum antimicrobial potential. A degradation efficiency of 95.73 % was achieved for methylene blue (MB) dye by photocatalysis under sunlight within 210 minutes. These findings demonstrate that ZnO NPs synthesized using *Swertia chirayita* exhibit excellent antimicrobial and photocatalytic properties, making them promising candidates for environmental remediation and biomedicine. This study underscores the potential of green synthesis approaches for developing sustainable nanomaterials.

Keywords: Antimicrobial activity, phytochemicals, photocatalytic degradation, zinc oxide nanoparticles

INTRODUCTION

Nanotechnology has made substantial advances in many fields, including medicine, environmental remediation, energy storage etc., owing to its capability to manipulate materials at the nanoscale (Abdol Aziz *et al.*, 2019). With this technological advancement, new nanomaterials with unique properties have been developed that are revolutionizing industries and applications (Rahman *et al.*, 2022). ZnO NPs are highly advantageous due to their large surface area, excellent photocatalytic activity, and notable antimicrobial properties, making them ideal for diverse applications (Muhammad *et al.*, 2019; J. Singh *et al.*, 2019). These characteristics make ZnO NPs highly suitable for uses like antimicrobial and antifungal activities (Dadi *et al.*, 2019), wastewater treatments and the degradation of environmental pollutants (Alharbi *et al.*, 2023; Mousa *et al.*, 2021).

The rising level of environmental pollution, as well as the emergence of antibiotic-resistant microorganisms, pose significant global challenges. In particular, water pollution due to industrial dye contaminants remains a major concern. Numerous industries, including paper, printing, leather, textiles, and pharmaceuticals, heavily rely on dyes. Textile dyeing and finishing processes produce up to 200,000 tonnes of dye waste per year through effluent (Abdullah *et al.*, 2022). These large-scale

dyes such as methylene blue (MB) pollute water supplies and pose health risks to humans and the environment (Batra *et al.*, 2022). Effluent dyes must be removed before discharge to protect water bodies. Photocatalytic degradation, particularly using nanomaterials such as ZnO NPs, has demonstrated significant potential for dye removal (López-López *et al.*, 2021). While ZnO NPs have many potential applications, conventional methods for synthesizing them often involve toxic chemicals and consume a lot of energy, which can negatively affect the environment and hinder sustainability (Herlekar *et al.*, 2014). In response to the environmental concerns associated with traditional nanoparticle synthesis methods, there has been a growing emphasis on green approaches (Weldegebrical, 2020). One such method employs natural plant extracts rich in bioactive compounds like alkaloids, polyphenols, proteins, flavonoids, sugars, and terpenoids to reduce the metal precursor and stabilize resulting nanoparticles (Barzinjy & Azeez, 2020). This innovative approach leverages the potential of plant-based compounds to mitigate the use of hazardous chemicals and enhance the performance of nanoparticles. Past research has explored the versatility of plant-mediated synthesis in producing ZnO NPs with diverse characteristics (Abomuti *et al.*, 2021).

This research emphasizes the eco-friendly synthesis of ZnO nanoparticles using zinc nitrate hexahydrate and the aqueous leaf extract of the plant *Swertia chirayita*. This plant is a member of the Gentianaceae family and is noted for its abundant phytochemicals, such as phenolics, flavonoids, and terpenoids (Swati *et al.*, 2023). These bioactive compounds act as natural agents for reduction and stabilization, promoting the eco-friendly synthesis of ZnO NPs and also enhancing their biocompatibility and potential for therapeutic applications. (K. Singh *et al.*, 2019). Additionally, *Swertia chirayita* has been widely utilized in traditional medicinal practices, which suggests its potential for producing biologically active nanoparticles with enhanced therapeutic properties. Unlike many other plant extracts, *Swertia chirayita* has been less explored for nanoparticle synthesis, offering a unique and eco-friendly methodology. Furthermore, the green synthesis method employed in this study avoids using noxious chemicals, aligning with the principles of green chemistry and providing an environmentally sustainable and cost-efficient alternative to conventional synthesis methods. This study aids the growing body of research on plant-mediated nanoparticle synthesis by highlighting the potential of *Swertia chirayita* for producing nanoparticles with applications in antimicrobial and environmental fields. This study aims to characterize the synthesized ZnO NPs. Their antimicrobial efficacy against strains of bacteria and fungi is evaluated. Additionally, the photocatalytic efficiency in degrading methylene blue (MB) dye under sunlight irradiation is assessed. By providing a sustainable alternative to conventional synthesis methods, this study seeks to address global challenges such as water pollution and antimicrobial resistance.

MATERIALS AND METHOD

Materials

This study utilized high-purity chemicals throughout the experiments. Zinc nitrate hexahydrate ($\text{Zn}(\text{NO}_3)_2 \cdot 6\text{H}_2\text{O}$, 99.5% purity) was obtained from Loba Chemical Pvt. Ltd. (Mumbai, India). Sodium hydroxide (NaOH, 97% purity) and methylene blue ($\text{C}_{16}\text{H}_{18}\text{ClN}_3\text{S}$) were purchased from Thermo Fisher Scientific India Pvt. Ltd. (India). Ethanol (99.9% purity) was obtained from RCP Distilleries India Pvt. Ltd. (Meerut, India). Double distilled water was employed as the solvent for all solution preparations.

Plant Extract Preparation

Fresh *Swertia chirayita* leaves were collected from Shadananda Municipality - 9, Bhojpur, Nepal. After thorough cleaning and 14 days of shade drying, the leaves were thoroughly crushed into a fine powder using a grinder. The resulting powder was subsequently stored in a sealed container to maintain its integrity and prevent contamination. ZnO nanoparticles were synthesized using 2 % aqueous extract prepared by stirring at 60°C for 1 hour, followed by filtration. The extract was stored at 4°C for subsequent use in various applications.

Synthesis of ZnO Nanoparticles

The synthesis of ZnO NPs was carried out with slight modifications to the procedure outlined by Barzinjy & Azeez (Barzinjy & Azeez, 2020). 4 g of $\text{Zn}(\text{NO}_3)_2 \cdot 6\text{H}_2\text{O}$ was dissolved in 100 mL of aqueous extract maintaining pH 10 with 0.1 NaOH and the mixture was subjected to continuous stirring for two hours at 60°C. The obtained precipitate was collected via centrifugation, rinsed thoroughly with ethyl alcohol and distilled water, and later dried at 80°C. Two hours of calcination at 400°C produced ZnO NPs. The synthesized nanoparticles were stored in an airtight container for subsequent analysis.

Phytochemical Analysis

A crude extract of *Swertia chirayita* was analysed qualitatively to detect the presence of various secondary metabolites, following established standard protocols (Aiyegoro & Okoh, 2010; Harborne, 1998).

Characterization of ZnO NPs

Several techniques were used to characterize ZnO nanoparticles synthesized. In order to examine the optical properties, a UV-visible spectrophotometer (SPECORD 200 PLUS, Analytik Jena, Germany) was used, with measurements taken across the wavelength range of 300–800 nm.

FTIR spectroscopy was performed to analyze and detect the functional groups present in the samples and understand their role in nanoparticle synthesis. The spectra were recorded using (IRTracer-100, SHIMADZU) across a wavenumber range of 4000–500 cm^{-1} .

The crystal structure of the synthesized ZnO nanoparticles was examined using an X-ray diffractometer (D2 Phaser, Bruker) with Cu $K\alpha$ radiation, scanning a 2θ range from 20° to 80°. The average crystallite size (D) was determined using the Debye-Scherrer equation (Patterson, 1939), expressed as:

$$D = \frac{k\lambda}{\beta \cos \theta} \quad (1)$$

In which, D represents crystallite size in nanometers, K is Scherrer constant (0.9), λ is the Wavelength of an incident X-ray (1.5406 Å), β is Full width at half maximum of peak (FWHM) in radians and θ is diffraction angle (radians).

The sample's surface morphology and elemental composition were examined using a JEOL JSM-6701F field emission scanning electron microscope (FESEM) coupled with energy-dispersive X-ray spectroscopy (EDS) and performed at the JBNU CURF EM Laboratory in Korea.

Photocatalytic Degradation Study

The photocatalytic effectiveness of produced ZnO NPs was assessed by studying the degradation of methylene

blue (MB) dye under specific conditions. Following the procedure outlined by Khadka *et al.*, the MB solution with a calculated amount of ZnO NPs was exposed to direct sunlight. The photocatalysis experiment involved adding 5 mg of ZnO NPs to 50 mL of a 4 ppm MB dye solution (Khadka *et al.*, 2024). For 30 minutes under dark conditions, the solution was agitated to assurance that the nanoparticles were well distributed and that MB was adsorbed onto their surface. The solution was left undisturbed for 30 minutes to achieve adsorption-desorption equilibrium. It was then exposed to direct sunlight from 11 AM to 3 PM. The reaction progress was monitored by periodically withdrawing a 3 mL aliquot. These samples were centrifuged for three minutes at 12,000 rpm. The residual dye concentration was analyzed with a UV-visible spectrophotometer, measuring absorbance in the 550–750 nm wavelength range. The dye degradation percentage was calculated using the following formula:

$$\text{Percentage of degradation} = \frac{(A_0 - A_t)}{A_0} \times 100 \quad (2)$$

Where A_0 represents the initial absorbance of the methylene blue (MB) dye solution, and A_t denotes the absorbance after a specific time interval t .

Antimicrobial Activity Study

To evaluate antimicrobial activity, the agar well diffusion method was employed against two bacterial strains, *Escherichia coli* (Gram-negative), *Staphylococcus aureus* (Gram-positive), and one fungus strain, *Candida albicans*.

Using a sterile cotton swab, 150 μL of each bacterial culture that had been cultivated in liquid broth (LB) media was spread out on the sterilized Mueller-Hinton Agar (MHA) plates. ZnO NPs sample plates (one dish per well) and a kanamycin standard (5 mg/mL, 10 μL) were added to wells. The zones of inhibition were evaluated to assess the antimicrobial efficacy following a 24-hour incubation period at 37°C.

RESULTS AND DISCUSSION

Phytochemical Screening

The phytochemical screening of the *Swertia chirayita* leaf extract was conducted to identify the presence of bioactive compounds that may play a role in the ZnO NPs production. These compounds consist of alkaloids, flavonoids, tannins, phenols, saponins, terpenoids etc. as shown in Table 1. These phytochemicals, particularly phenols and flavonoids, can act as natural reducing and stabilizing agents during the green synthesis of nanoparticles (Ahmad *et al.*, 2019). Additionally, these phytochemicals may contribute to the enhanced biological and catalytic properties of the synthesized nanoparticles. Flavonoids and tannins possess inherent antimicrobial properties, which, could enhance the bactericidal efficacy of ZnO NPs in targeting pathogenic microorganisms (Yagoub *et al.*, 2022). Additionally, these phytochemicals contribute significantly to enhancing the photocatalytic activity of the synthesized ZnO nanoparticles (Mousa *et al.*, 2024). Their presence contributes to the overall efficiency and functionality of the nanoparticles in photocatalytic applications.

Table 1. Phytochemical analysis of *Swertia chirayita* extract

Phytochemical constituents	Tests	Results
Flavonoids	NaOH and acid test	+
	Mg ribbon test	+
Alkaloids	Mayer test	+
	Wagner test	+
Saponins	Froth Test	+
Terpenoids	Salkowaski test	+
Quinone	5% NaOH test	-
Tannins	Lead acetate test	+
Phenolic	FeCl ₃ test	+

* + indicates the presence and – indicates the absence

Synthesis of ZnO NPs

The formation of ZnO NPs was evidenced by a visual colour change in solution, attributed to the surface plasmon resonance (SPR) phenomenon which is characteristic of nanoparticles. The suspension was centrifuged, washed with distilled water and ethanol, dried, and calcined at 400°C to obtain the ZnO NPs. The calcination at 400°C ensures the complete decomposition of organic residues from the leaf extract and promotes the crystallization of ZnO NPs. This step is crucial for enhancing the purity, crystallinity, and stability of the nanoparticles, all of which are important

for their functional characteristics in various applications.

The exact mechanism behind the green synthesis of ZnO NPs using plant extracts is not fully understood. One possible mechanism suggests that phytochemicals reduce Zn^{2+} ions to zinc atoms (Zn^0), which subsequently react with dissolved oxygen in the solution to create ZnO nuclei. Furthermore, these phytochemicals may serve as capping and stabilizing agents, helping to maintain the stability of the nanoparticles (Baral *et al.*, 2025; Fouda *et al.*, 2023). Another proposed mechanism involves the formation of

metal-coordinated complexes between the phytochemicals and zinc ions. When subjected to thermal treatment, these complexes decompose, promoting the formation of ZnO NPs that are stabilized and capped by the phytochemicals from the extract (Fouda *et al.*, 2023; Mongy & Shalaby, 2024).

UV-visible Spectroscopic Analysis

Using UV-visible spectroscopy, the optical properties were examined. The absorption spectrum (Figure 2a) showed a prominent absorption peak centred at 376 nm. This peak, which represents ZnO's band gap absorption, indicates that ZnO NPs were successfully synthesized. According to Aldabahi *et al.* this peak results from the transfer of electrons from O-2p orbitals to Zn-3d orbital (Aldabahi *et al.*, 2020). The band gap energy (E_g) was determined using the Tauc plot technique.

$$(\alpha h\nu)^{1/\gamma} = A (h\nu - E_g) \quad (3)$$

where α = absorption coefficient, h = Planck's constant, ν = photon frequency, A = constant and $\gamma = 1/2$ for direct band gap semiconductors (Viezbicke *et al.*, 2015).

For ZnO NPs, it can be measured by plotting $(\alpha h\nu)^2$ against $h\nu$ and extrapolating the linear region of the plot to the x-axis (Vindhya *et al.*, 2023). The obtained band gap value was 2.92 eV (Figure 2b) which is suitable for visible light absorption. This underscores the ability of the synthesized ZnO nanoparticles to efficiently degrade dyes through photocatalysis. The calculated band gap energy aligns well with values reported in earlier studies (MuthuKathija *et al.*, 2023) confirming the consistency and reliability of the results. This may be due to defect states introduced by the phytochemicals present in leaf extract and their role in controlling nanoparticle size during formation (Shaba *et al.*, 2021; Sharma *et al.*, 2022). The purity of synthesized nanoparticles is indicated by the sharp, intense peak without any additional peaks in the absorption spectrum.

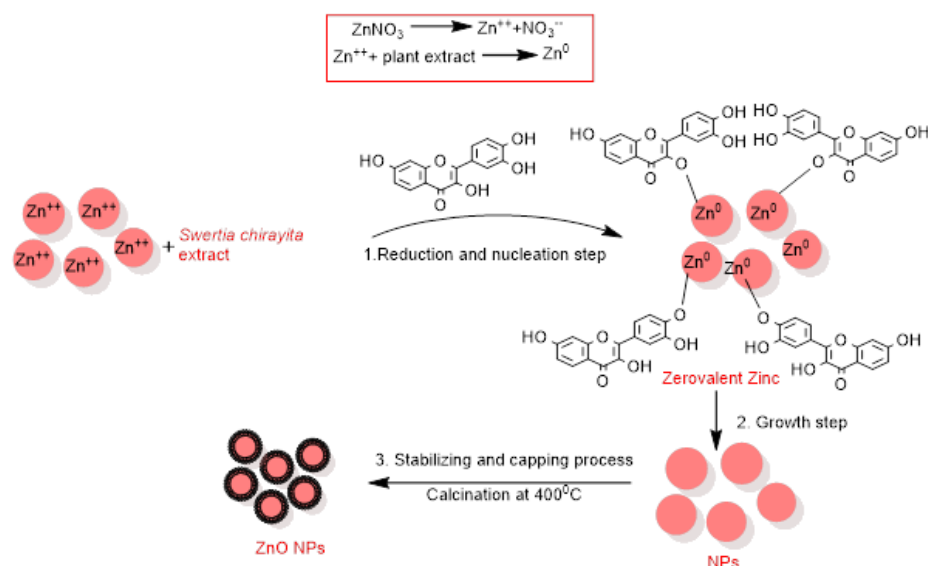


Figure 1. Proposed mechanism of green synthesis of ZnO NPs using *Sweritia chirayita* aqueous leaf extract

To clarify the molecular interactions between the leaf extract and the ZnO NPs, FTIR analysis was carried out. The functional groups detected are likely responsible for capping and stabilizing the nanoparticles, playing a crucial role in maintaining their structure and preventing aggregation. The resulting FTIR spectra of the ZnO NPs and leaf extract are shown in Fig. 3. It displays distinct absorption bands at wavenumbers 698, 877, 1083, 1171, 1427, 2878 and 3375 cm^{-1} for the ZnO NPs, and, 1042, 1405, 1589, 2878 and 3360 cm^{-1} for the leaf extract. The broad absorption peaks around 3360 cm^{-1} (extract) and 3375 cm^{-1} (ZnO NPs) are likely attributed to O-H stretching vibrations, suggesting the presence of biomolecules like flavonoids, terpenoids, and

polyphenols (Hamza *et al.*, 2022; Jamdagni *et al.*, 2018). The minor peak at 2878 cm^{-1} in both spectra is attributed to C-H stretching vibrations of alkanes (El-Khawaga *et al.*, 2023).

The band at 1042 cm^{-1} is characteristic of the C-O stretching vibration of alcohol or phenol groups. The presence of these groups suggests the involvement of hydroxyl-rich compounds in the extract (Jamdagni *et al.*, 2018). The band at 1405 cm^{-1} signifies C-H bending and the 1589 cm^{-1} band corresponds to C=C stretching vibrations in aromatics, indicating polyphenolic compounds (Rahman *et al.*, 2022). The intense peak at 1427 cm^{-1} in the ZnO NPs spectrum, absent in the plant

extract, suggests that it is associated with nanoparticle formation. This peak is likely due to C-O stretching vibrations, which may arise from phenolic or other organic compounds in the plant extract interacting with the ZnO surface. The intensity changes and peak position shifts observed in the FTIR spectra suggest significant interactions between biomolecules' functional groups and the surface of the ZnO nanoparticles. These interactions likely facilitate the capping and stabilization of nanoparticles during green synthesis, as commonly observed in biosynthesized nanomaterials (Abdullahi Ari *et al.*, 2023). Additionally, the minor peaks between 500 to 700 cm^{-1} are ascribed to out-of-plane bending vibrations of C-H bonds, typically associated with aromatic compounds, which are

prevalent in plant extracts (Kalaba *et al.*, 2024; Yashni *et al.*, 2021). The distinct peak at 877 cm^{-1} is attributed to C-O-S stretching (Coates, 2006; Fouda *et al.*, 2023). The appearance of characteristic peaks in the 450-700 cm^{-1} range, corresponding to the stretching vibrations of Zn-O bonds, confirms the successful synthesis of ZnO nanoparticles. These peaks are absent in the spectrum of the leaf extract, indicating that they are specific to the ZnO nanostructure (Muhammad *et al.*, 2019; Naseer *et al.*, 2020). These results suggest that organic functional groups played a key role in stabilizing and capping the ZnO nanoparticles, likely improving their properties.

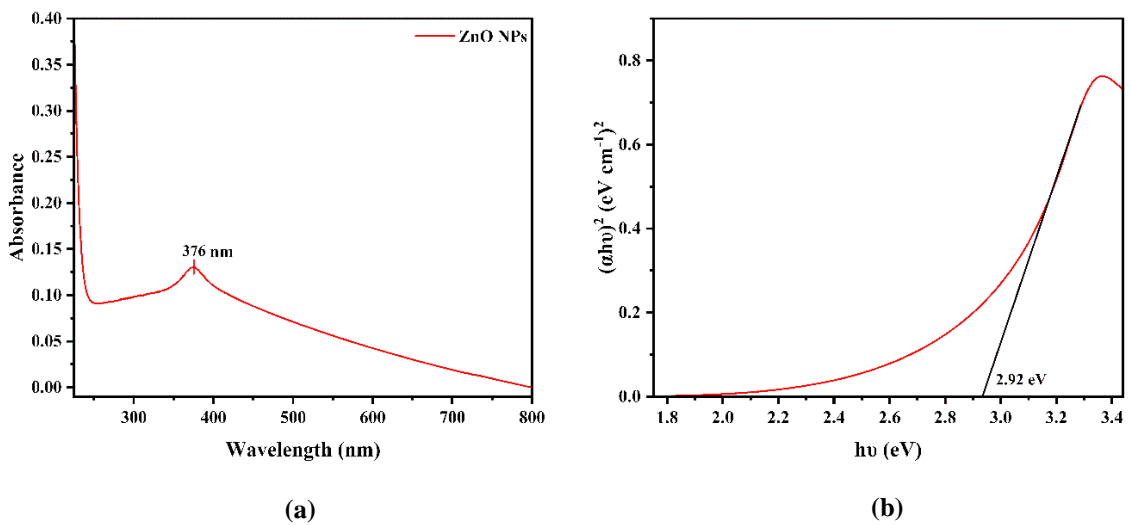


Figure 2. (a) Absorbance spectrum (b) Tauc plot with a band gap of ZnO NPs FTIR analysis

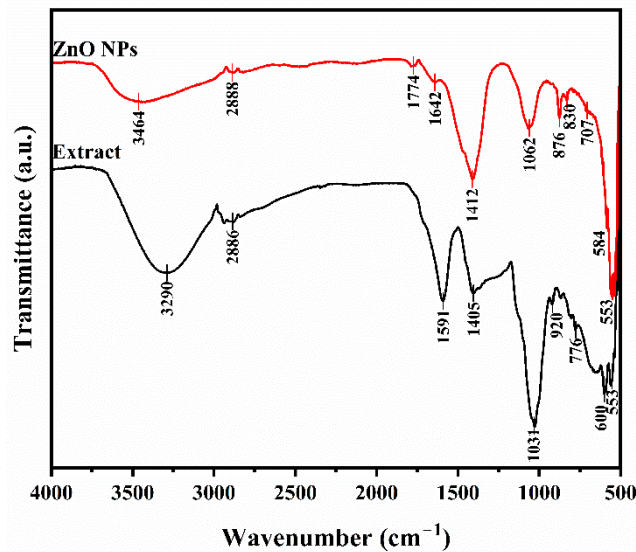


Figure 3. FTIR spectra of extract of *Swertia chirayita* and ZnO NPs

XRD Analysis

XRD patterns of ZnO NPs are presented in Figure 4. XRD analysis determined their phase purity, crystallite size, and lattice parameters. The presence of intense and sharp peaks confirms its highly crystalline nature. The synthesized ZnO NPs exhibited diffraction peaks at 2θ values of 31.49° , 34.08° , 35.92° , 47.27° , 56.41° , 62.59° , 66.03° , 67.62° , 68.76° , 72.28° and 77.70° corresponding to the lattice planes (h, k, l) of (100), (002), (101), (102), (110), (103), (200), (112), (201), (004), and (202) respectively.

The detected diffraction peaks correspond to the hexagonal wurtzite structure of ZnO (JCPDS card no. 00-036-1451), indicating the high crystallinity and phase purity of the synthesized nanoparticles (K. Singh *et al.*, 2019). These results closely match previously documented results (Azizi *et al.*, 2016; Faisal *et al.*, 2021; Maheo *et al.*, 2023). The average crystallite size, determined based on the broadening of the (101) peak,

was found to be 10.88 nm. No additional peaks confirm their high purity.

Morphological and Elemental Characterization: SEM and EDS Analysis

This scanning electron microscopy (SEM) image provides structural and morphological details of the sample under analysis. Figure 5 (a) revealed well-dispersed nanoparticles with predominantly spherical or quasi-spherical particles with some degree of agglomeration. The particle size distribution was analyzed using Image J software, resulting in the histogram displayed in Figure 5 (b). The results show an average nanoparticle size of 21.89 nm with a relatively narrow distribution. Minor variations in size may be due to differences in nucleation and growth rates during the green synthesis process. Such a morphology could indicate a nanoparticle network or a material with a high surface area, potentially suitable for applications like photocatalysis (Sachin *et al.*, 2023).

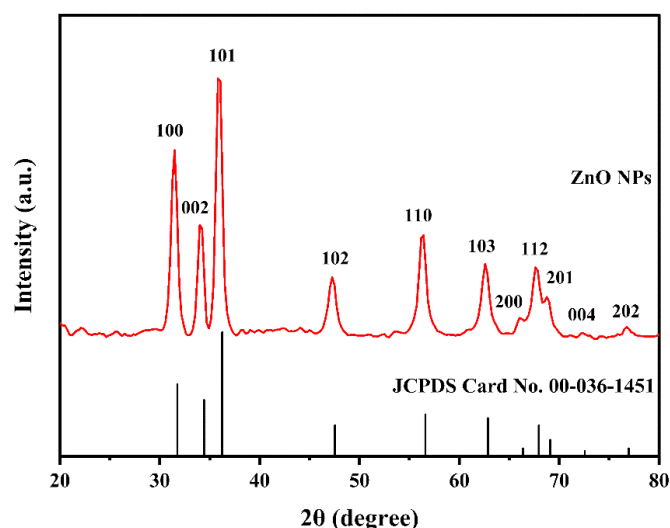


Figure 4. XRD patterns of ZnO NPs

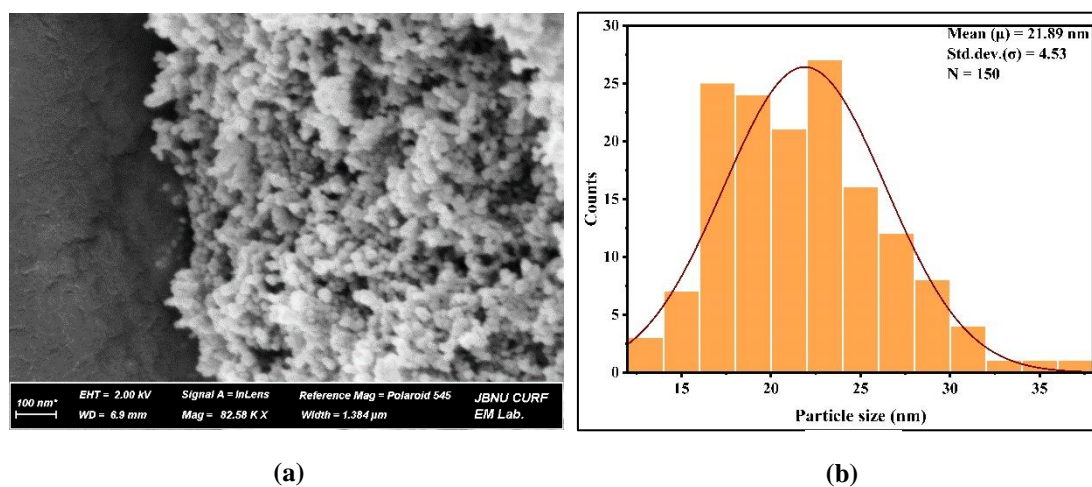


Figure 5. (a) SEM image of ZnO NPs at a magnification of 82.58 K \times (b) histogram showing average particle size distribution

The EDS analysis of the synthesized ZnO NPs provides crucial insights into the elemental composition. The EDS spectrum is presented in Figure 6. This spectrum confirmed the elemental composition, comprising a weight % of 58.05% zinc (Zn), 26.65% oxygen (O), and 15.30% carbon (C), with an atomic % of 26.77% (Zn), 43.40% (O), and 29.83% (C) respectively. The peak at around 1 keV corresponds to Zn $L\alpha$, and the peak at around 0.5 keV and 0.3 keV corresponds to O $K\alpha$ and C $K\alpha$ respectively confirming the presence of these elements (Alharbi *et al.*, 2023). The high zinc and oxygen content indicates the successful synthesis of ZnO NPs.

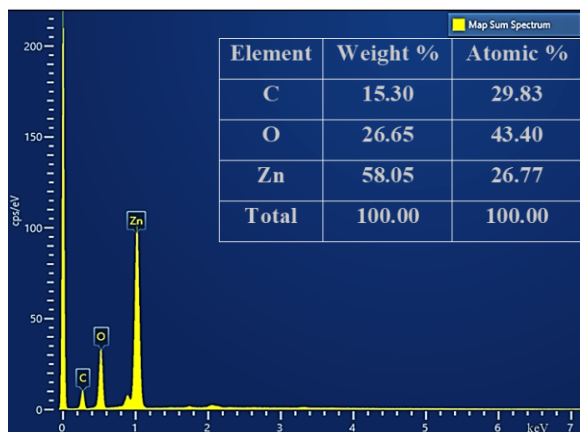


Figure 6. EDS map sum spectrum of ZnO NPs with a table showing elemental composition (in inset)

The higher zinc content compared to the ideal stoichiometric ratio suggests a zinc-rich composition, which may indicate the presence of oxygen vacancies or a deviation from the expected ZnO stoichiometry. This could contribute to enhanced photocatalytic properties of the nanoparticles, as oxygen vacancies are known to

influence the electronic structure and reactivity of ZnO. The presence of carbon may be ascribed to the organic residues from the leaf extract or from the carbon tape normally used to prepare the SEM samples.

To further support this, the FTIR results indicate the presence of aromatic phenolic and other functional groups associated with organic compounds from the leaf extract. These findings align with the existence of carbon and confirm the role of phytochemicals in the synthesis and stabilization of the nanoparticles. The XRD analysis supports these results. No additional peaks indicate the purity, with no significant contamination from other elements and successful synthesis of ZnO NPs.

Photocatalytic Degradation Activity

The photocatalytic activity of synthesized ZnO NPs was assessed by monitoring MB dye degradation under sunlight exposure at various time intervals, without continuous stirring. Figure 7(a) shows the absorption spectra of MB degradation, with the absorbance decreasing over time. A significant reduction of absorbance peak at 664 nm indicates the breakdown of MB dye as exposure time increases. The results showed a gradual increase in degradation efficiency, reaching approximately 95.73% after 210 minutes of irradiation, as illustrated in Figure 7(b).

These findings highlight the excellent photocatalytic activity of *Swertia chirayita*-mediated ZnO NPs. The phytochemicals act as capping agents, improving the dispersion and stability of the NPs, which increases the active surface area available for photocatalytic reactions. Additionally, they may contribute to bandgap modulation, enabling better absorption of visible light (Shaba *et al.*, 2021).

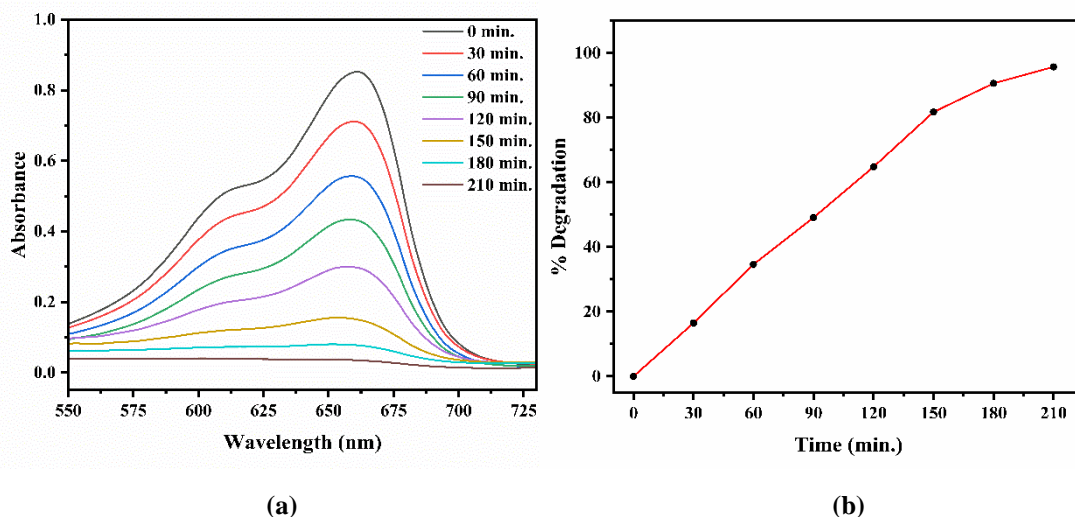
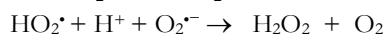
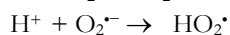
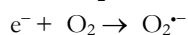
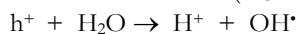
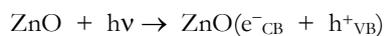


Figure 7. (a) Photodegradation of MB under sunlight irradiation (b) Percentage degradation of MB with time

This process involves light-induced photoexcitation of electrons in ZnO NPs, generating electron-hole pairs that drive redox reactions for organic pollutant

degradation. These electron-hole pairs interact with H_2O and O_2 molecules, producing highly reactive oxygen species (ROS) such as hydroxyl radicals (OH^\bullet) and

superoxide anions ($O_2^{\bullet -}$), which are responsible for the oxidative breakdown of MB molecules (Zong *et al.*, 2014). This process effectively converts MB into water, carbon dioxide, and minerals (Hanif *et al.*, 2019; Zong *et al.*, 2014).



The kinetics of MB degradation using synthesized ZnO NPs under photocatalytic conditions was studied. The degradation kinetics were assessed by plotting $\ln(C_0/C_t)$ against time, as shown in Figure 8. The linear relationship is indicative of pseudo-first-order kinetics, expressed as:

$$\ln(C_0/C_t) = kt \quad (4)$$

Here, C_0 represents the initial concentration, C_t denotes the concentration at time t , and k is the rate constant. The slope of the plot of $\ln(C_0/C_t)$ against the time gives a rate constant, k . The linearity of the plot ($R^2 = 0.9839$) validates the suitability of the pseudo-first-order model for describing MB degradation under the given experimental conditions as shown in Figure 8. The calculated rate constant (k) was 0.0085 min^{-1} .

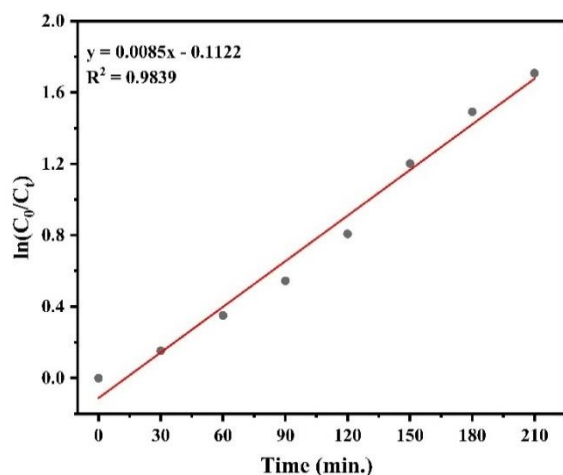


Figure 8. Pseudo-first-order kinetic plot for MB degradation

The use of *Swertia chirayita* for ZnO nanoparticle synthesis offers notable economic and environmental benefits. This green synthesis technique offers a sustainable and economical alternative to conventional chemical methods by minimizing the use of toxic reagents and energy consumption. *Swertia chirayita*, a widely available medicinal plant, supports biodiversity utilization and reduces the overall cost of nanoparticle production.

From an environmental perspective, plant-mediated synthesis minimizes hazardous byproducts, aligns with green chemistry principles, and supports eco-friendly applications, especially in wastewater treatment. The biodegradable nature of plant-based stabilizing agents further enhances the sustainability of the process. Additionally, the ZnO NPs synthesized using *Swertia chirayita* exhibit strong photocatalytic activity, particularly in the degradation of organic dyes like MB. This photocatalytic capability not only highlights the potential of these nanoparticles in environmental remediation but also underscores their application in water purification, making this approach highly beneficial for sustainable, eco-friendly solutions.

Antimicrobial Activity Study

The antimicrobial activity was evaluated against aqueous leaf extract of the *Swertia chirayita* and the standard antibiotic kanamycin. The results, presented in Figure 9 and Table 2, display the zones of inhibition (ZOI) indicating antimicrobial efficacy. ZnO NPs demonstrated considerable antimicrobial efficacy against all tested strains. The observed inhibition zones were larger than those produced by the extract, indicating enhanced antimicrobial activity of the synthesized ZnO NPs. All tested strains showed clear zones of inhibition, indicating the broad-spectrum potential of ZnO NPs. The negative control (50 % Dimethyl sulphoxide, DMSO) showed no inhibition, confirming that the observed effects were due to the antimicrobial agents tested. This may be due to the adsorption of biologically active phytochemicals from the *Swertia chirayita* onto the surface of ZnO NPs, which, together with the nanoparticles, inhibited the growth of the tested strains. The antibacterial activity is mainly attributed to their capability to generate reactive oxygen species (ROS), which cause oxidative stress in bacterial cells. This stress can lead to membrane disruption, protein denaturation, and DNA fragmentation (Jalal *et al.*, 2010). Additionally, the release of Zn^{2+} ions (Li *et al.*, 2011) and the direct interaction of nanoparticles with bacterial cell walls causes loss of cell integrity (Zhang *et al.*, 2007).

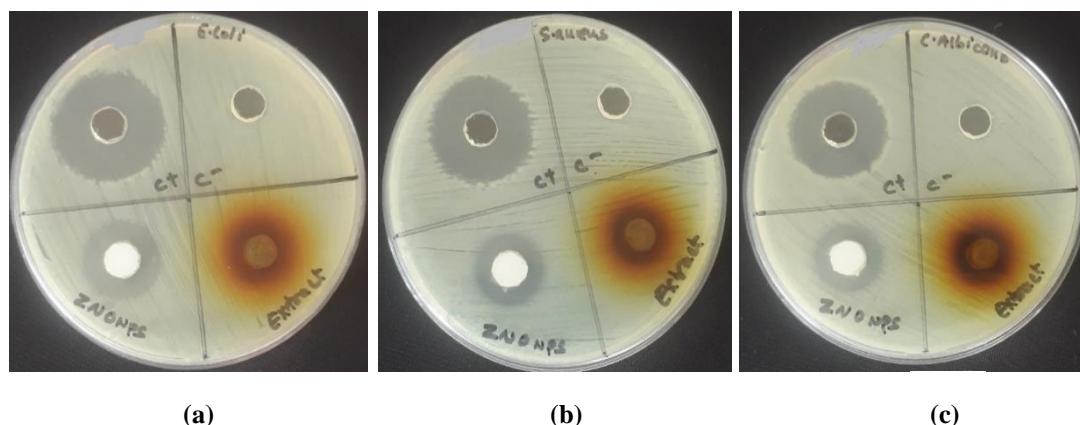


Figure 9. Antimicrobial activity of ZnO NPs against (a) *Escherichia coli* (b) *Staphylococcus aureus* (c) *Candida albicans*

Table 2. Zones of inhibition of ZnO NPs, plant extract, and positive control against tested bacterial and fungal strains

Strain	Reference culture	Type	Positive control (c ⁺) (mm)	ZnO NPS (mm)	Extract (mm)
<i>Escherichia coli</i>	ATCC 8739	Gram -ve	26	18	12
<i>Staphylococcus aureus</i>	ATCC 6538P	Gram +ve	23	17	12
<i>Candida albicans</i>	ATCC 2091	Fungi	25	17	12

CONCLUSIONS

This study demonstrates the successful green synthesis of ZnO NPs involving *Swertia chirayita* leaf extract. They were characterized using UV-vis, XRD, FTIR, and FESEM with EDS spectroscopy. XRD confirmed their crystalline nature with a hexagonal wurtzite structure and an average crystallite size of 10.88 nm. A strong absorption peak at 376 nm in the UV-vis spectrum evidences the formation of ZnO NPs. FTIR analysis identified functional groups in the leaf extract that aided in nanoparticle synthesis and stabilization. The FESEM-EDS analysis confirmed the well-dispersed nanoparticles with predominantly spherical morphology and a high weight percentage of zinc and oxygen. The synthesized nanoparticles exhibited significant antimicrobial activity against both bacterial and fungal pathogens. Furthermore, they demonstrated high photocatalytic efficiency (95.73%) in degrading MB dye under sunlight irradiation within 210 minutes. These findings show the promise of *Swertia chirayita*-mediated ZnO NPs for antimicrobial and environmental remediation applications. For scalability, future research should focus on optimizing synthesis and degradation parameters, evaluating the long-term stability and reusability of these nanoparticles for industrial-scale applications in wastewater treatment and antimicrobial fields assessing the commercial feasibility of *Swertia chirayita* for the large-

scale production of nanoparticles, including scalability, cost-effectiveness, and sustainable cultivation practices.

ACKNOWLEDGEMENTS

The authors are grateful to the Central Department of Chemistry, Tribhuvan University, Kirtipur, Kathmandu, Nepal and the Department of Chemistry, Tri-Chandra Multiple Campus, Tribhuvan University, Kathmandu, Nepal for providing laboratory facilities and the Himalaya Research Institute of Biotechnology Pvt. Ltd., Bhaktapur, Nepal for antimicrobial assay.

AUTHOR CONTRIBUTIONS

DK, PB: designed the study, collected samples, performed the laboratory work and wrote the manuscript; JB, SKG: designed the study, analyzed data and reviewed the manuscript; BPB, BRP, MRP: designed the study, supervised, analyzed the data, reviewed and finalized the manuscript.

CONFLICT OF INTEREST

The authors declare no conflict of interests.

DATA AVAILABILITY STATEMENT

The data that supports the findings of this study are available from the corresponding author, upon reasonable request.

REFERENCES

- Abdol Aziz, R.A., Abd Karim, S.F., & Rosli, N.A. (2019). The effect of pH on zinc oxide nanoparticles characteristics synthesized from banana peel extract. *Key Engineering Materials*, 797, 271–279. <https://doi.org/10.4028/www.scientific.net/KEM.797.271>.
- Abdullah, F.H., Bakar, N.H.H.A., & Bakar, M.A. (2022). Current advancements on the fabrication, modification, and industrial application of zinc oxide as photocatalyst in the removal of organic and inorganic contaminants in aquatic systems. *Journal of Hazardous Materials*, 424, 127416. <https://doi.org/10.1016/j.jhazmat.2021.127416>.
- Abdullahi Ari, H., Adewole, A.O., Ugya, A.Y., Asipita, O.H., Musa, M.A., & Feng, W. (2023). Biogenic fabrication and enhanced photocatalytic degradation of tetracycline by bio structured ZnO nanoparticles. *Environmental Technology*, 44(9), 1351–1366. <https://doi.org/10.1080/09593330.2021.2001049>.
- Abomuti, M.A., Danish, E.Y., Firoz, A., Hasan, N., & Malik, M.A. (2021). Green synthesis of zinc oxide nanoparticles using *Salvia officinalis* leaf extract and their photocatalytic and antifungal activities. *Biology*, 10(11), 1075. <https://doi.org/10.3390/biology10111075>.
- Ahmad, T., Bustam, M.A., Irfan, M., Moniruzzaman, M., Asghar, H.M.A., & Bhattacharjee, S. (2019). Mechanistic investigation of phytochemicals involved in green synthesis of gold nanoparticles using aqueous *Elaeis guineensis* leaves extract: Role of phenolic compounds and flavonoids. *Biotechnology and Applied Biochemistry*, 66(4), 698–708. <https://doi.org/10.1002/bab.1787>.
- Aiyegoro, O.A., & Okoh, A.I. (2010). Preliminary phytochemical screening and In vitro antioxidant activities of the aqueous extract of *Helichrysum longifolium* DC. *BMC Complementary and Alternative Medicine*, 10(1), 21. <https://doi.org/10.1186/1472-6882-10-21>.
- Aldalbahi, A., Alterary, S., Ali Abdullrahman Almoghim, R., Awad, M.A., Aldosari, N.S., Fahad Alghannam, S., Nasser Alabdan, A., Alharbi, S., Ali Mohammed Alateeq, B., Abdulrahman Al Mohsen, A., Alkathiri, M.A., & Abdulrahman Alrashed, R. (2020). Greener synthesis of zinc oxide nanoparticles: characterization and multifaceted applications. *Molecules*, 25(18), 4198. <https://doi.org/10.3390/molecules25184198>.
- Alharbi, F.N., Abaker, Z.M., & Makawi, S.Z.A. (2023). Phytochemical substances—mediated synthesis of zinc oxide nanoparticles (ZnO NPS). *Inorganics*, 11(8), 328. <https://doi.org/10.3390/inorganics11080328>.
- Azizi, S., Mohamad, R., Bahadoran, A., Bayat, S., Rahim, R.A., Ariff, A., & Saad, W.Z. (2016). Effect of annealing temperature on antimicrobial and structural properties of bio-synthesized zinc oxide nanoparticles using flower extract of *Anchusa italica*. *Journal of Photochemistry and Photobiology B: Biology*, 161, 441–449. <https://doi.org/10.1016/j.jphotobiol.2016.06.007>.
- Baral, J., Pokharel, N., Dhungana, S., Tiwari, L., Khadka, D., Pokhrel, M.R., & Poudel, B.R. (2025). Green synthesis of copper oxide nanoparticles using *Mentha* (mint) leaves characterization and its antimicrobial properties with phytochemicals screening. *Journal of Nepal Chemical Society*, 45(1), 111–121. <https://doi.org/10.3126/jncs.v45i1.74491>.
- Barzinjy, A.A., & Azeez, H.H. (2020). Green synthesis and characterization of zinc oxide nanoparticles using *Eucalyptus globulus* Labill. leaf extract and zinc nitrate hexahydrate salt. *JN Applied Sciences*, 2(5), 991. <https://doi.org/10.1007/s42452-020-2813-1>.
- Batra, V., Kaur, I., Pathania, D., Sonu, & Chaudhary, V. (2022). Efficient dye degradation strategies using green synthesized ZnO-based nanoplatfroms: A review. *Applied Surface Science Advances*, 11, 100314. <https://doi.org/10.1016/j.apsadv.2022.100314>.
- Coates, J. (2006). Interpretation of infrared spectra, A practical approach. In *Encyclopedia of Analytical Chemistry*. Wiley. <https://doi.org/10.1002/9780470027318.a5606>.
- Dadi, R., Azouani, R., Traore, M., Mielcarek, C., & Kanaev, A. (2019). Antibacterial activity of ZnO and CuO nanoparticles against Gram positive and Gram negative strains. *Materials Science and Engineering: C*, 104, 109968. <https://doi.org/10.1016/j.msec.2019.109968>.
- El-Khawaga, A.M., Elsayed, M.A., Gobara, M., Suliman, A.A., Hashem, A.H., Zaher, A.A., Mohsen, M., & Salem, S.S. (2023). Green synthesized ZnO nanoparticles by *Saccharomyces cerevisiae* and their antibacterial activity and photocatalytic degradation. *Biomass Conversion and Biorefinery*, 15, 2673–2684. <https://doi.org/10.1007/s13399-023-04827-0>.
- Faisal, S., Jan, H., Shah, S.A., Shah, S., Khan, A., Akbar, M.T., Rizwan, M., Jan, F., Wajidullah, Akhtar, N., Khattak, A., & Syed, S. (2021). Green synthesis of zinc oxide (ZnO) nanoparticles using aqueous fruit extracts of *Myristica fragrans*: their characterizations and biological and environmental applications. *ACS Omega*, 6(14), 9709–9722. <https://doi.org/10.1021/acsomega.1c00310>.
- Fouda, A., Saied, E., Eid, A.M., Kouadri, F., Alemam, A.M., Hamza, M.F., Alharbi, M., Elkesh, A., & Hassan, S.E.-D. (2023). Green synthesis of zinc oxide nanoparticles using an aqueous extract of *Punica granatum* for antimicrobial and catalytic activity. *Journal of Functional Biomaterials*, 14(4), 205. <https://doi.org/10.3390/jfb14040205>.
- Hamza, M.F., Wei, Y., Althumayri, K., Fouda, A., & Hamad, N.A. (2022). Synthesis and characterization of functionalized chitosan nanoparticles with pyrimidine derivative for enhancing ion sorption and application for removal of contaminants. *Materials*, 15(13), 4676. <https://doi.org/10.3390/ma15134676>.
- Hanif, M., Lee, I., Akter, J., Islam, M., Zahid, A., Sapkota, K., & Hahn, J. (2019). Enhanced photocatalytic and antibacterial performance of ZnO nanoparticles prepared by an efficient thermolysis

- method. *Catalysts*, 9(7), 608. <https://doi.org/10.3390/catal9070608>.
- Harborne, J.B. (1998). *Phytochemical methods a guide to modern techniques of plant analysis (Third Edition)*. Chapman & Hall.
- Herlekar, M., Barve, S., & Kumar, R. (2014). Plant-mediated green synthesis of iron nanoparticles. *Journal of Nanoparticles*, 2014, 1–9. <https://doi.org/10.1155/2014/140614>.
- Jalal, R., Goharshadi, E.K., Abareshi, M., Moosavi, M., Yousefi, A., & Nancarrow, P. (2010). ZnO nanofluids: Green synthesis, characterization, and antibacterial activity. *Materials Chemistry and Physics*, 121(1–2), 198–201. <https://doi.org/10.1016/j.matchemphys.2010.01.020>.
- Jamdagni, P., Khatri, P., & Rana, J.S. (2018). Green synthesis of zinc oxide nanoparticles using flower extract of *Nyctanthes arbor-tristis* and their antifungal activity. *Journal of King Saud University - Science*, 30(2), 168–175. <https://doi.org/10.1016/j.jksus.2016.10.002>.
- Kalaba, M.H., El-Sherbiny, G.M., Ewais, E.A., Darwesh, O.M., & Moghannem, S.A. (2024). Green synthesis of zinc oxide nanoparticles (ZnO-NPs) by *Streptomyces baarnensis* and its active metabolite (Ka): a promising combination against multidrug-resistant ESKAPE pathogens and cytotoxicity. *BMC Microbiology*, 24(1), 254. <https://doi.org/10.1186/s12866-024-03392-4>.
- Khadka, D., Gautam, P., Dahal, R., Ashie, M.D., Paudyal, H., Ghimire, K.N., Pant, B., Poudel, B.R., Bastakoti, B.P., & Pokhrel, M.R. (2024). Evaluating the photocatalytic activity of green synthesized iron oxide nanoparticles. *Catalysts*, 14(11), 751. <https://doi.org/10.3390/catal14110751>.
- Li, M., Zhu, L., & Lin, D. (2011). Toxicity of ZnO nanoparticles to *Escherichia coli*: mechanism and the influence of medium components. *Environmental Science & Technology*, 45(5), 1977–1983. <https://doi.org/10.1021/es102624t>.
- López-López, J., Tejada-Ochoa, A., López-Beltrán, A., Herrera-Ramírez, J., & Méndez-Herrera, P. (2021). Sunlight photocatalytic performance of ZnO nanoparticles synthesized by green chemistry using different botanical extracts and zinc acetate as a precursor. *Molecules*, 27(1), 6. <https://doi.org/10.3390/molecules27010006>.
- Maheo, A.R., Vithiya B, S.M., Arul Prasad T, A., Mangesh, V.L., Perumal, T., Al-Qahtani, W.H., & Govindasamy, M. (2023). Cytotoxic, antidiabetic, and antioxidant study of biogenically improvised *Elsholtzia blanda* and chitosan-assisted zinc oxide nanoparticles. *ACS Omega*, 8(12), 10954–10967. <https://doi.org/10.1021/acsomega.2c07530>.
- Mongy, Y., & Shalaby, T. (2024). Green synthesis of zinc oxide nanoparticles using *Rhus coriaria* extract and their anticancer activity against triple-negative breast cancer cells. *Scientific Reports*, 14(1), 13470. <https://doi.org/10.1038/s41598-024-63258-7>.
- Mousa, H.M., Alenezi, J.F., Mohamed, I.M.A., Yasin, A.S., Hashem, A.-F.M., & Abdal-hay, A. (2021). Synthesis of TiO₂@ZnO heterojunction for dye photodegradation and wastewater treatment. *Journal of Alloys and Compounds*, 886, 161169. <https://doi.org/10.1016/j.jallcom.2021.161169>.
- Mousa, S.A., Wissa, D.A., Hassan, H.H., Ebnalwaled, A.A., & Khairy, S.A. (2024). Enhanced photocatalytic activity of green synthesized zinc oxide nanoparticles using low-cost plant extracts. *Scientific Reports*, 14(1), 16713. <https://doi.org/10.1038/s41598-024-66975-1>.
- Muhammad, W., Ullah, N., Haroon, M., & Abbasi, B.H. (2019). Optical, morphological and biological analysis of zinc oxide nanoparticles (ZnO NPs) using *Papaver somniferum* L. *RSC Advances*, 9(51), 29541–29548. <https://doi.org/10.1039/C9RA04424H>.
- MuthuKathija, M., Sheik Muhideen Badhusha, M., & Rama, V. (2023). Green synthesis of zinc oxide nanoparticles using *Pisonia alba* leaf extract and its antibacterial activity. *Applied Surface Science Advances*, 15, 100400. <https://doi.org/10.1016/j.apsadv.2023.100400>.
- Naseer, M., Aslam, U., Khalid, B., & Chen, B. (2020). Green route to synthesize Zinc Oxide Nanoparticles using leaf extracts of *Cassia fistula* and *Melia azadirach* and their antibacterial potential. *Scientific Reports*, 10(1), 9055. <https://doi.org/10.1038/s41598-020-65949-3>.
- Patterson, A.L. (1939). The Scherrer Formula for X-Ray Particle Size Determination. *Physical Review*, 56(10), 978–982. <https://doi.org/10.1103/PhysRev.56.978>.
- Rahman, F., Majed Patwary, M.A., Bakar Siddique, M.A., Bashar, M.S., Haque, M.A., Akter, B., Rashid, R., Haque, M.A., & Royhan Uddin, A.K.M. (2022). Green synthesis of zinc oxide nanoparticles using *Cocos nucifera* leaf extract: characterization, antimicrobial, antioxidant and photocatalytic activity. *Royal Society Open Science*, 9(11). <https://doi.org/10.1098/rsos.220858>.
- Sachin, J., Singh, N., Singh, R., Shah, K., & Pramanik, B.K. (2023). Green synthesis of zinc oxide nanoparticles using lychee peel and its application in anti-bacterial properties and CR dye removal from wastewater. *Chemosphere*, 327, 138497. <https://doi.org/10.1016/j.chemosphere.2023.138497>.
- Shaba, E.Y., Jacob, J.O., Tijani, J.O., & Suleiman, M.A.T. (2021). A critical review of synthesis parameters affecting the properties of zinc oxide nanoparticle and its application in wastewater treatment. *Applied Water Science*, 11(2), 48. <https://doi.org/10.1007/s13201-021-01370-z>.
- Sharma, P., Dhungana, S., Rai, R., Khadka, D., Hitan, D. K., Pokhrel, M.R., Gautam, S.K., & Poudel, B.R. (2022). Temperature dependent synthesis of zinc sulphide (ZnS) nanoparticles and its characterization. *Amrit Research Journal*, 3(01), 67–74. <https://doi.org/10.3126/arj.v3i01.50498>.
- Singh, J., Kumar, S., Alok, A., Upadhyay, S.K., Rawat, M., Tsang, D.C.W., Bolan, N., & Kim, K.-H. (2019). The potential of green synthesized zinc oxide

- nanoparticles as nutrient source for plant growth. *Journal of Cleaner Production*, 214, 1061–1070. <https://doi.org/10.1016/j.jclepro.2019.01.018>.
- Singh, K., Singh, J., & Rawat, M. (2019). Green synthesis of zinc oxide nanoparticles using *Punica granatum* leaf extract and its application towards photocatalytic degradation of Coomassie brilliant blue R-250 dye. *SN Applied Sciences*, 1(6), 624. <https://doi.org/10.1007/s42452-019-0610-5>.
- Swati, K., Bhatt, V., Sendri, N., Bhatt, P., & Bhandari, P. (2023). *Swertia chirayita*: A comprehensive review on traditional uses, phytochemistry, quality assessment and pharmacology. *Journal of Ethnopharmacology*, 300, 115714. <https://doi.org/10.1016/j.jep.2022.115714>.
- Viezbicke, B.D., Patel, S., Davis, B.E., & Birnie, D.P. (2015). Evaluation of the Tauc method for optical absorption edge determination: ZnO thin films as a model system. *Physica Status Solidi (B)*, 252(8), 1700–1710. <https://doi.org/10.1002/pssb.201552007>.
- Vindhya, P.S., Suresh, S., Kunjikannan, R., & Kavitha, V.T. (2023). Antimicrobial, antioxidant, cytotoxicity and photocatalytic performance of Co doped ZnO nanoparticles biosynthesized using *Annona Muricata* leaf extract. *Journal of Environmental Health Science and Engineering*, 21(1), 167–185. <https://doi.org/10.1007/s40201-023-00851-4>.
- Weldegebrical, G.K. (2020). Synthesis method, antibacterial and photocatalytic activity of ZnO nanoparticles for azo dyes in wastewater treatment: A review. *Inorganic Chemistry Communications*, 120, 108140. <https://doi.org/10.1016/j.inoche.2020.108140>.
- Yagoub, A.E.A., Al-Shammari, G.M., Al-Harbi, L.N., Subash-Babu, P., Elsayim, R., Mohammed, M.A., Yahya, M.A., & Fattiny, S.Z.A. (2022). Antimicrobial properties of zinc oxide nanoparticles synthesized from *Lavandula pubescens* shoot methanol extract. *Applied Sciences*, 12(22), 11613. <https://doi.org/10.3390/app122211613>.
- Yashni, G., Al-Gheethi, A., Radin Mohamed, R.M.S., Dai-Viet, N.V., Al-Kahtani, A.A., Al-Sahari, M., Nor Hazhar, N.J., Noman, E., & Alkhadher, S. (2021). Bio-inspired ZnO NPs synthesized from *Citrus sinensis* peels extract for Congo red removal from textile wastewater via photocatalysis: optimization, mechanisms, techno-economic analysis. *Chemosphere*, 281, 130661. <https://doi.org/10.1016/j.chemosphere.2021.130661>.
- Zhang, L., Jiang, Y., Ding, Y., Povey, M., & York, D. (2007). Investigation into the antibacterial behaviour of suspensions of ZnO nanoparticles (ZnO nanofluids). *Journal of Nanoparticle Research*, 9(3), 479–489. <https://doi.org/10.1007/s11051-006-9150-1>.
- Zong, Y., Li, Z., Wang, X., Ma, J., & Men, Y. (2014). Synthesis and high photocatalytic activity of Eu-doped ZnO nanoparticles. *Ceramics International*, 40(7), 10375–10382. <https://doi.org/10.1016/j.ceramint.2014.02.123>.